Research Article

Mohamed Nfaoui*, Walid Abouloifa, Sanaa Hayani-Mounir, Mohamed Yassine Roboa, Khalil El-hami

Shading impact on the electricity generated by a photovoltaic installation using "Solar Shadow-Mask"

https://doi.org/10.1515/EHS-2023-0048
received April 09, 2023; accepted February 25, 2024

Abstract: Solar energy is an excellent source of renewable power, but designing photovoltaic (PV) systems can be challenging without proper knowledge of solar radiation. The amount of energy received at the installation site plays a crucial role in determining the number of panels required to meet the electrical demand. For a given electrical demand, higher levels of received energy imply a reduced number of panels required, and vice versa. Hence, having knowledge of this irradiance is of paramount importance in the design and sizing of solar energy systems. The primary objective of this article is to provide an accurate estimation of electricity production in a PV installation when it is affected by shading. To achieve this, we performed calculations of the irradiation (direct and diffuse) received by our installation using the "Hottel" method, which integrates relevant local site parameters for our study. Subsequently, we study the impact of shading by conducting shade mask measurements on our installation. This enables us to obtain an accurate estimation of the irradiance received by the PV panels. The measurements include surveys of the geometry of obstacles and shade measurements taken at various times of the day. Additionally, a practical study of shading effects will be conducted using "close shading masks." This method was applied to a 1.44 kW_p PV installation located at the Faculty of Science and Technology of Settat (Morocco), where the output energy of PV panels was calculated. Finally, the effect of shading on the PV installation was quantified.

Keywords: photovoltaic, shading, solar radiation, system, electricity production

*** Corresponding author: Mohamed Nfaoui,** Multidisciplinary Laboratory of Research and Innovation (LaMRI), EMAFI Team, Polydisciplinary Faculty, University of Sultan Moulay Slimane, Khouribga, Morocco, e-mail: nfaoui.smp@gmail.com
Walid Abouloifa: Multidisciplinary Laboratory of Research and Innovation (LaMRI), EMAFI Team, Polydisciplinary Faculty, University of Sultan Moulay Slimane, Khouribga, Morocco, e-mail: walidabouloifa@gmail.com
Sanaa Hayani-Mounir: Multidisciplinary Laboratory of Research and Innovation (LaMRI), EMAFI Team, Polydisciplinary Faculty, University of Sultan Moulay Slimane, Khouribga, Morocco, e-mail: sanaachikhi@yahoo.fr
Mohamed Yassine Roboa: Multidisciplinary Laboratory of Research and Innovation (LaMRI), EMAFI Team, Polydisciplinary Faculty, University of Sultan Moulay Slimane, Khouribga, Morocco, e-mail: mohamed.yassine.roboa@gmail.com
Khalil El-hami: Scientific Institute, Mohammed V University in Rabat, Av. Ibn Batouta, BP 703, 10106 Rabat, Morocco, e-mail: elhami_k@yahoo.com

Nomenclature

Indices

PV	photovoltaic
α	the tilt angle
S	available module surface (m^2)
J	the order of the day number in the year

Elements of solar time

σ	this parameter designates the sunshine
t & T	t is the fraction of the time during which the sky is clear and T is the total duration of the day
AH	hour angle of the sunrise or sunset
t_{ls}	sunrise time
t_{cs}	sunset time

Elements of solar energy

H_h	global energy received by the sky whose veiling is defined by unit of horizontal surface
H_{hc}	energy received under the same conditions of measurements but by clear sky
H_0	energy received by a surface arranged horizontally, outside the atmosphere
H_{diff}	diffuse energy received

Elements of coordinate systems

H	angle of the solar height – elevation
Z	the zenith angle
$\vec{I}$	the unit vector carried by the direction of the solar rays
$\vec{n}$	the unit vector carried by the normal to the surface
θ	angle of incidence, the angle between $(\vec{I}, \vec{n})$

Elements of power radiation

I_{t}	power received on the ground by a horizontal surface
I_0	solar constant outside atmosphere
I_{h}	global power radiation received on the capture area
I_{dir}	direct power radiation received on the capture area
I_{diff}	diffuse power radiation received on the capture area

Elements of energy concept

k_{t}	indices of clarity
$R_{\mathrm{dir}\cdot\alpha}$	the correction factor relative to diffuse radiation
M	the relative length of the path traveled by the sun's rays through the atmosphere
O	optical depth
A	apparent extraterrestrial flux
R_{dir}	quantity called tilt factor

Elements of PV installation

E	monthly or annual electricity production (kW h)
G	monthly or annual irradiation received on the PV installation
η_{global}	overall efficiency of the installation

1 Introduction

The production of energy is a challenge of great importance in the years to come. On the other hand, the energy needs of industrialized societies are steadily increasing. Indeed, developing countries will need more and more energy to carry out their development (Vasiliev et al. 2019). Today, most of the world's energy production comes from fossil sources. By contrast, a so-called renewable energy must regenerate naturally and indefinitely on the temporal scale of our civilization.

Among these energies, the solar energy currently meets these criteria of both abundance at the Earth's surface and infinite regeneration at our scale. Indeed, the development of profitable and economically viable conversion systems necessarily goes through the understanding of the various components of the system at their head, the solar panel. The latter is composed of several solar cells that require study and understanding (Cooper 1969, Nfaoui et al. 2023).

Our work is based on the study of a photovoltaic (PV) pumping installation at the Faculty of Science and Technology (FST) of Settat (Morocco); the PV panels are placed on a concrete support in the garden of the establishment (Nfaoui and El-hami 2018).

This installation comprises 12 monocrystalline silicon PV panels of 120 W_c each, an area of 9.9696 m^2 and a power of 1.44 kW_c. These panels, oriented west-east and inclined at 32°, connect to the pump to irrigate the green areas and all plants of the establishment.

In winter, when the sun is particularly low, garden trees create a drop shadow on the first line of the modules of the installation. Modules are wired in series; this has the effect of reducing the electrical production of this line. At first, we made a theoretical study of our installation estimating its annual production and the losses due to the shading phenomenon, and then we compared with the results that will be obtained if the installation is well positioned.

2 Power and energy received by a capture surface

2.1 Hottel's method

There are many ways to calculate the solar radiation received on Earth (Tiwari 2004, Tiwari and Barnwal 2008, Kasten and Young 1989, Nfaoui et al. 2021). In a simplified manner, the Hottel's method reads the average value of the power received on the ground, by a horizontal surface, visibility used by meteorologists, and coefficients that include atmospheric conditions at the

altitude of the site. Certainly, when the solar radiation collection surface possesses a specific orientation and inclination, it becomes imperative to adjust the mathematical equations provided by the Hottel method by incorporating coefficients that consider the actual conditions of inclination and orientation in real-world applications (Islahi et al. 2015, Taşçıoğlu et al. 2016).

The power received on the ground by a horizontal surface is given by the following relationship:

$$I_t = a_0 \cdot \sin(h) \cdot \{a_0 + a_1 \cdot \exp(-a_2/\sin(h))\}, \quad (1)$$

where h is the angle of the solar height (elevation) and the coefficients a_0, a_1, and a_2 are dependent on visibility:

$$\begin{cases} a_0 = 0.4237 - 0.008200 \cdot (6 - z)^2 \\ a_1 = 0.5055 + 0.00595 \cdot (6.5 - z)^2 \\ a_2 = 0.2711 - 0.01858 \cdot (2.5 - z)^2 \end{cases}$$

for altitudes less than 2.5 km,

$$\begin{cases} a_0 = 0.2538 - 0.0063 \cdot (6 - z)^2 \\ a_1 = 0.7678 + 0.001 \cdot (6.5 - z)^2 \\ a_2 = 0.249 - 0.081 \cdot (2.5 - z)^2 \end{cases}$$

for an urban haze atmosphere.

It should be noted that this method allows the interpolation, for a given altitude, of the coefficients in the abovementioned visibility range.

Some similar models consider that the atmosphere is transparent and keeps its optical properties constant through the different parameters and coefficients of the models.

The atmospheric conditions, particularly cloud coverage, are inherently uncertain, with the sky being either fully or partially covered for a given duration. One common approach for determining the extent of cloud coverage is to perform visual estimates of the obscured portion of the sky at regular intervals. However, this method relies on human observation and therefore, may result in significant variability and inaccuracies in measurements.

This parameter quantifies the duration of sunshine. It is defined as the fraction, "t," of the clear sky duration over the total duration of daylight, "T," from sunrise to sunset. The expression for sunshine can be represented as

$$\sigma = t/T \text{ it is obvious that: } 0 \le \sigma \le 1.$$

If we know the hour angle AH of the sunrise or sunset (compared to the local noon), the total duration of the day can be calculated as follows:

$$T = 2 \cdot \mathrm{AH}/15, \quad (2)$$

$$\sigma = (15/(2 \cdot \mathrm{AH})) \cdot t. \quad (3)$$

Several researchers have attempted to establish a linear relationship between insolation and radiation through linear mathematical equations. The most widely used correlations belong to two types: Angstrom-type relationships, which only consider local site conditions (where σ represents insolation), and Angstrom-Black relationships, which take into account the solar constant.

$$H_\mathrm{h} = H_\mathrm{hc} \cdot (a_0 + a_1 \cdot \sigma) \left[\frac{\mathrm{J}}{\mathrm{m}^2\,\mathrm{day}}\right] : \text{Angstrom-type}, \quad (4)$$

$$H_\mathrm{h} = H_0 \cdot (b_1 + b_2 \cdot \sigma) \left[\frac{\mathrm{J}}{\mathrm{m}^2\,\mathrm{day}}\right] : \text{Angstrom-Black-type}, \quad (5)$$

with

$$\mathrm{H}_0 = \int_{t_\mathrm{ls}}^{t_\mathrm{cs}} I_0 \cdot \sin(h)\,\mathrm{d}(t), \quad (6)$$

where t is the solar (or local) time, t_cs is the sunset time, and t_ls is the sunrise time.

These regressions are all based on large series of daily measurements of sunshine which can be used directly to have daily correlations or grouped into monthly classes represented by their average, when using them, specify the data used: Daily, monthly, or yearly (Tables 1 and 2).

The values of Tables 1 and 2 gave us the results shown in Table 3, relating to the city of Casablanca according to Angstrom Black.

For applications requiring the determination of instantaneous values of power or energy, other

Table 2: Annual average of b_1 and b_2

Coeff.	The annual average on b_1	The annual average on b_2
Casablanca	0.288	0.448

Table 1: Values of b_1 and b_2 obtained by linear regression for the regions of Casablanca (Tiwari 2004)

Coeff.	Jan	Feb	Mar	Apr	May	Jun	Jul	Aug	Sept	Oct	Nov	Dec
b_1	0.23	0.29	0.25	0.32	0.30	0.31	0.40	0.37	0.38	0.21	0.22	0.17
b_2	0.49	0.45	0.53	0.44	0.47	0.45	0.34	0.36	0.32	0.52	0.48	0.52

Table 3: Values of H_h according to Angstrom Black's relationship for the city of Casablanca

Month	σ	H_h (Joule/m^2 day)
Jan	0.60	12,454,194
Feb	0.66	12,608,628
Mar	0.75	12,685,845
Apr	0.84	13,071,931
May	0.95	12,685,845
Jun	1.00	12,917,496
Jul	1.00	13,071,931
Aug	1.00	12,840,279
Sep	0.89	12,068,108
Oct	0.74	12,299,760
Nov	0.61	12,299,760
Dec	0.58	11,990,891
Average	0.81	12,531,411

approaches such as the types of indices of clarity k_t are to be considered

$$k_t = f\left(\frac{I_h}{I_0}, h\right) \quad \text{whether} \quad k_t = I_h \cdot \sin(h)/I_0, \tag{7}$$

or

$$k_t = f\left(\frac{H_h}{H_0}\right) \text{whether } k_t = H_h/H_0, \tag{8}$$

or

$$k_t = f\left(\frac{I_{diff}}{I_h}\right) \text{whether } k_t = I_{diff}/I_0, \tag{9}$$

or

$$k_t = f\left(\frac{H_{diff}}{H_h}\right) \text{whether } k_t = H_{diff}/H_h. \tag{10}$$

We note that, in general, the regressions on the mean values have a linear dependence whereas the correlations on the daily values are of the third and the fourth degree in k_t.

We quote the example of correlation on the daily values of the Maghreb countries.

$$k_t = H_{diff}/H_0,$$

for the Arab Maghreb: Morocco, Algeria, and Tunisia.

$$\frac{H_{diff}}{H_h} = -0.759 + 5.869 \cdot k_t - 8.884 \cdot k_t^2 + 3.590 \cdot k_t^3. \tag{11}$$

We justify these dispersions by the means used: Measuring instruments and the various reflectivities due to the ground, neighborhoods, and meteorological data (pollution, cloud, humidity, and dust).

The correlation of instantaneous power values is based on the assumption that the flux and irradiance are uniform and remain relatively constant over time intervals of approximately 1 h. This assumption is justified by the low solar elevation during this time period. The definition of the clearness index takes into account the height of the sun, which results in a nearly instantaneous correction over time.

$$k_t = \frac{I_{diff}}{I_h} \cdot \sin(h). \tag{12}$$

But the diffuse is determined from the direct I_{dir} and the global I_h; that is to say

$$I_{diff} = I_h - I_{dir}.$$

So,

$$k_t = \frac{I_h - I_{dir}}{I_h} \cdot \sin(h) = \left(1 - \frac{I_{dir}}{I_h}\right) \cdot \sin(h). \tag{13}$$

3 Study of solar radiation received on ground surface "CLEAR DAY"

The power or energy received by a surface is dependent on several factors according to its orientation, its inclination on the other hand is composed of the same basic solar elements which are the direct, diffuse, and reflected irradiation (Nfaoui and El-hami 2018).

3.1 Solar position and solar angles – angle of incidence ("ω")

The position of the sun is defined by its height h and its azimuth φ measured with respect to the South. And the

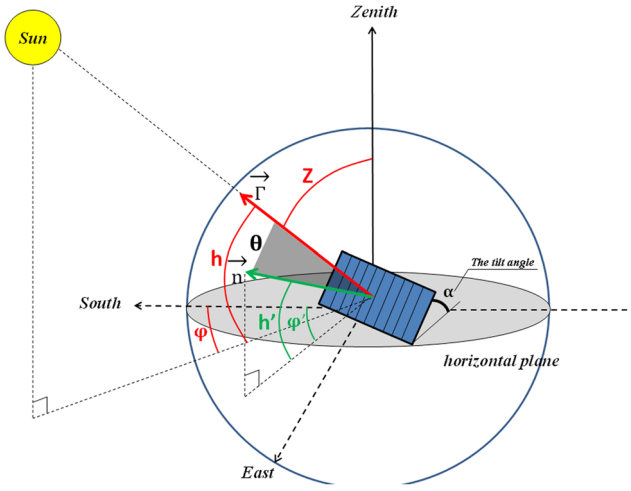

Figure 1: The solar horizontal coordinates and the angle of incidence. www.sciencedirect.com/science/article/pii/S2352484717301725.

plane of the solar panel is oriented toward south at an angle φ' and is inclined at the tilt angle α relative to the ground (Figure 1).

The angle of incidence of the solar beam with any surface of inclination and orientation is the angle formed by the direction vector of the solar beam and the normal leaving the surface (Nfaoui and El-hami 2018).

3.2 Direct solar radiation

The direct solar radiation estimated on inclined surface without being diffused by the atmosphere is given by (Ennaoui 2014, Oudrane et al. 2017, Schimot et al. 2010):

$$I_{\mathrm{dir}\cdot\alpha\cdot\varphi} = \frac{I_{\mathrm{t}}}{\sin(h)}\cdot\cos(\theta) \tag{14}$$

$$= \frac{I_{\mathrm{t}}}{\sin(h)}\cdot\{\cos(h)\cos(\varphi - \varphi')\sin(Z') + \sin(h)\sin(Z')\}.$$

Usually, we note R_{dir} by the quantity called tilt factor:

$$R_{\mathrm{dir}\cdot\alpha\cdot\varphi} = \frac{\cos(h)\cos(\varphi - \varphi')\sin(Z') + \sin(h)\sin(Z')}{\sin(h)} \tag{15}$$

$$\Rightarrow I_{\mathrm{dir}\cdot\alpha\cdot\varphi} = R_{\mathrm{dir}\cdot\beta\cdot\gamma}\cdot I_{\mathrm{t}}.$$

The received power on the capture area is given by

$$I_{\mathrm{dir}} = A\cdot\exp(-K\cdot m). \tag{16}$$

This is an amount that includes the geographic parameters of the system and the astronomical data of the sun in its movement.

$$A = 1{,}160 + 75\sin\left(\frac{360}{365}(j - 275)\right)\cdot \mathrm{W/m^2}, \tag{17}$$

$$K = 0.175 + 0.035\sin\left(\frac{360}{365}(j - 100)\right), \tag{18}$$

$$m = \frac{1}{\sin(h)}. \tag{19}$$

3.3 Diffused radiation

The hypothesis posits that diffuse radiation is uniformly distributed in the sky and can be represented as an infinite plane. This assumption enables the computation of the correction factor $R_{\mathrm{dir}\cdot\alpha}$ with respect to diffuse radiation, once the inclination angle has been established (Nfaoui and El-hami 2018, Ennaoui 2014).

$$R_{\mathrm{dif}.\alpha} = \frac{1 + \cos(\alpha)}{2}. \tag{20}$$

The power received on a capture area is

$$I_{\mathrm{dif}} = \mathrm{C}\cdot I_{\mathrm{Dir}}\cdot R_{\mathrm{dif}}, \tag{21}$$

$$C = 0.095 + 0.04\sin\left(\frac{360}{365}(j - 100)\right). \tag{22}$$

The implementation of this formula gives a clear idea about the different values of energy daily, monthly, and yearly.

4 Slar irradiation received on the surface of our installation

The geographical features of the study site have been identified for Settat city in Morocco (located at latitude 33.029° and longitude –7.619°). The direct, diffuse, and global irradiation levels are estimated on a daily and monthly basis, taking into account the inclination and orientation of the PV installation, which is 32° and West-East (270°), respectively (Nfaoui and El-hami 2018).

We have developed a MATLAB code that calculates and tracks the daily irradiation of the typical days of each month for our installation in Settat city. For more information on solar radiation calculation, refer the paper "Optimal tilt angle and orientation for solar PV arrays: case of Settat city in Morocco (Nfaoui et al. 2023, Nfaoui and El-hami 2018)."

4.1 Daily distribution of solar irradiation and cumulative energy for each month of the year

The distribution of daily values of solar irradiation was calculated for the whole year, a finer analysis is to make this calculation month by month. We find the different components of solar radiation calculated over the year; it is assumed that the sky is very clear in the days of the year.

We have therefore plotted curves based on calculation models using a MATLAB code which calculates and traces the monthly irradiation, which were established for the Settat city, and then we added tables giving the annual variations of the monthly averages of the direct, diffuse, and global irradiations, indicating the monthly maximum and minimum of the whole year.

The evaluation of the cumulative monthly energy, in 1 month on the inclined and oriented surface, is done by a simple integral of the power.

We used the classical method, which uses power calculation expressions, to calculate the solar energy received, and then develop a MATLAB code that calculates and traces the evolution of cumulative monthly solar energy (Figure 2).

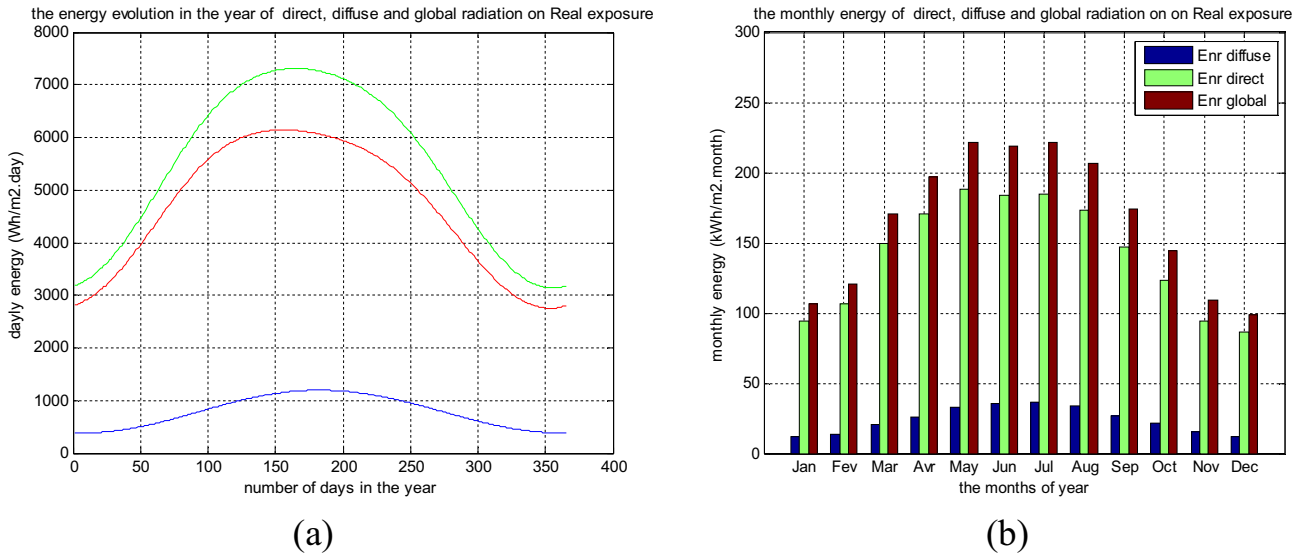

Figure 2: (a) Annual distribution of daily irradiation and (b) the monthly energy for the two modes of positions.

Figure 2a represents the monthly irradiation of the daily sums of solar radiation received relative to these positions (32° inclination and the west orientation [270°]) according to the months of the year in (W h/(m^2 day)). In Figure 2b, we represent the energy of the solar radiation calculated for the site of Settat city.

A summary of the results is given in the tables below.

4.2 Results of the calculations

The monthly variation in daily solar radiation is regular for the whole year (Figure 2).

The monthly maxima not only correspond to the days of the maximum duration of the day (the lowest values in December–January, and the highest in June–July) but also to that of the atmospheric mass $\left(m = \frac{1}{\sin(h)}\right)$. The quantity of direct radiation reaching the ground is influenced by the air mass (m). During winter, when the sun's altitude (h) is lower, the extended path of solar rays traversing through the atmosphere leads to heightened attenuation.

The monthly minima correspond to the days of the months of January and December (3,200 W h/m^2 day) and the absolute maximum in May and June (7,300 W h/m^2 day).

The tabulated results in Table 4, which numerically represent the data depicted in Figure 2, illustrate the annual and monthly distribution of solar irradiation. This data offers insights into the accumulation of energy distribution for each month. As depicted in Figure 2a, a minor peak exceeding 200 kW h/m^2 is evident during the summer months, characterized by the longest sunny days of the year. Conversely, the value drops below 120 kW h/m^2 during the winter months, indicating a significant seasonal effect. This seasonal variation is highlighted by the clustering of bars in the histogram shown in Figure 2(b), with each group representing a four-month season:

- Those of the summer: May, June, July, August > 200 kW h/m^2:
- Those of winter: November, December, January, February < 120 kW h/m^2
- Intermediate: March, April, September, October.'

Through this representation the annual global energy received on the plan of our installation is 1988.9 kW h/m^2.

Table 4: Monthly and annual irradiation received on our installation (kW h/m^2)

Months	Direct irradiation	Diffuse irradiation	Total irradiation
Jan	12.16	94.04	106.2
Feb	13.59	106.90	120.49
Mar	20.45	149.98	170.43
Apr	26.31	170.41	196.72
May	33.12	188.36	221.48
Jun	35.40	183.77	219.17
Jul	36.64	184.88	221.52
Aug	33.39	172.99	206.38
Sep	26.89	147.05	173.94
Oct	21.18	123.45	144.63
Nov	14.99	94.54	109.53
Dec	12.26	86.09	98.35
Whole year	286.38	1702.5	1988.88

4.3 Sunshine tables

The generation of electricity by a solar panel is dependent on the amount of solar irradiance at the installation site. A precise knowledge of the solar insolation characteristics is crucial in the design of a PV system.

We thus obtain two tables of solar irradiation: diffuse and global irradiation, respectively (Tables 5 and 6), received on 1 m^2 of our installation. We can represent the daily average values for each month of the year according to the notion of time, in the real case without shading them from the previous shadow mask, and we deduce the table of sunshine for the installation in the real case with the shadow of the ridge (Tables 5 and 6).

5 Study of the influence of shading on the productivity of our PV installation

To perform optimally, a solar PV system must undergo least possible shading, within that context, there are several investigations conducted in order to understand how to limit the influence of shading on PV productivity (Schimot et al. 2010, Chowdhury and Saha 2010, Bayraka et al. 2017). However, some constraints related to the place of installation (presence of mountain, trees, chimney, and electric pole) cannot be avoided. Mask is any obstacle hiding the PV modules from the sunlight (Sarniak 2020, Hashim et al. 2021).

5.1 Shading effects on our photovoltaic installation

In the state where we found the installation, the modules are oriented west at an inclination of 32° relative to the horizontal. PV panels placed on a roof and influenced by a set of obstacles (trees, pole, etc.) which creates remarkable shading on the PV cells (Figure 3) (El Iysaouy et al. 2016, Dolara et al. 2013).

5.1.1 General hypothesis

When a shadow appears on a PV module, it is considered, because of the wiring, that all the modules of the installation receive only diffuse radiation.

Table 5: Diffuse solar irradiation received on the surface of our installation (W h/m^2)

	Jan	Feb	Mar	Apr	May	Jun	July	Aug	Sep	Oct	Nov	Dec
05:00-05:30	0	0	0	0	0	0.20	1.59	0	0	0	0	0
05:30-06:00	0	0	0	0	3.15	5.31	2.37	0.03	0	0	0	0
06:00-06:30	0	0	0	3.81	13.89	17.86	12.84	5.52	0.68	1.06	0	0
06:30-07:00	0	0	1.98	14.28	26.24	29.63	26.49	18.40	8.99	2.26	0.07	0
07:00-07:30	0	0.85	9.81	24.96	33.91	37.09	35.53	30.29	22.30	11.35	2.70	0
07:30-08:00	2.61	7.01	19.53	31.26	38.73	41.96	41.32	37.53	31.25	22.20	10.78	3.57
08:00-08:30	9.58	15.68	25.52	35.08	41.95	45.31	45.22	42.15	36.54	28.53	19.14	11.18
08:30-09:00	16.49	20.85	28.93	37.58	44.21	47.71	47.97	45.28	39.92	32.26	23.80	17.35
09:00-09:30	19.68	23.72	31.07	39.30	45.84	49.47	49.96	47.48	42.21	34.65	26.53	20.70
09:30-10:00	21.72	25.49	32.49	40.53	47.04	50.77	51.44	49.06	43.81	36.25	28.29	22.69
10:00-10:30	23.01	26.64	33.48	41.41	47.91	51.74	52.52	50.22	44.94	37.35	29.45	23.96
10:30-11:00	23.85	27.42	34.17	42.04	48.55	52.44	53.32	51.05	45.74	38.102	30.21	24.79
11:00-11:30	24.40	27.95	34.64	42.47	48.99	52.94	53.88	51.64	46.27	38.59	30.71	25.33
11:30-12:00	24.76	28.29	34.95	42.74	49.26	53.25	54.25	52.01	46.60	38.87	30.98	25.65
12:00-12:30	24.97	28.48	35.11	42.87	49.39	53.41	54.44	52.20	46.74	38.96	31.08	25.79
12:30-13:00	25.08	28.54	35.17	42.94	49.46	53.48	54.52	52.28	46.83	39.05	31.16	25.87
13:00-13:30	25.12	28.60	35.21	42.94	49.48	53.49	54.55	52.30	46.79	38.96	31.08	25.86
13:30-14:00	25.03	28.54	35.13	42.81	49.29	53.34	54.42	52.15	46.59	38.70	30.83	25.69
14:00-14:30	24.73	28.35	34.92	42.55	48.99	53.04	54.12	51.83	46.20	38.24	30.38	25.35
14:30-14:00	24.34	28.02	34.57	42.14	48.52	52.56	53.65	51.32	45.59	37.55	29.69	24.80
14:00-14:30	23.74	27.52	34.05	41.54	47.86	51.88	52.96	50.58	44.72	36.54	28.68	23.98
14:30-15:00	22.87	26.83	33.32	40.72	46.96	50.96	52.03	49.56	43.51	35.11	27.23	22.80
15:00-15:30	21.62	25.76	32.29	39.59	45.75	49.72	50.77	48.17	41.84	33.09	25.14	21.08
15:30-16:00	19.81	24.29	30.85	38.04	44.12	48.08	49.09	46.28	39.51	30.20	21.83	18.35
16:00-16:30	15.58	22.21	28.83	35.90	41.91	45.87	46.83	43.70	36.21	24.44	8.32	6.33
16:30-17:00	2.48	16.67	25.90	32.88	38.85	42.89	43.75	40.09	30.65	7.27	7.20	0
17:00-17:30	0	1.63	16.23	28.01	34.45	38.70	39.44	34.63	14.46	0.03	0	0
17:30-18:00	0	0	0.32	10.75	25.78	32.27	32.73	20.90	0.67	0	0	0
18:00-18:30	0	0	0	0.03	4.13	15.82	15.27	1.83	0	0	0	0
18:30-19:00	0	0	0	0	0	0.04	0.03	0	0	0	0	0

Table 6: Global solar irradiation received on the surface of our installation (W h/m^2)

	Jan	Febr	Mar	Apr	May	Jun	Jul	Aug	Sept	Oct	Nov	Dec
05:00-05:30	0	0	0	0	0	0.20	1.59	0	0	0	0	0
05:30-06:00	0	0	0	0	3.15	5.31	2.37	0.03	0	0	0	0
06:00-06:30	0	0	0	3.82	26.24	29.64	12.84	5.53	0.69	2.27	0	0
06:30-07:00	0	0	1.98	14.28	33.91	37.09	26.49	18.41	9.00	11.36	0	0
07:00-07:30	2.60	3.86	9.82	24.96	38.73	41.97	35.54	30.29	22.31	22.21	2.70	0
07:30-08:00	9.58	7.01	19.53	31.27	41.96	45.32	41.32	37.54	31.26	28.53	10.78	3.57
08:00-08:30	16.19	15.68	25.52	35.08	70.57	81.75	45.23	42.16	36.55	32.27	19.14	11.18
08:30-09:00	19.68	20.85	28.93	39.48	119.31	128.31	68.22	47.20	39.93	36.67	23.81	17.35
09:00-09:30	21.71	23.72	32.27	77.52	169.58	176.31	114.48	90.75	63.97	81.22	26.55	20.70
09:30-10:00	36.56	25.72	66.20	130.51	219.78	224.27	162.59	140.87	115.59	132.67	39.03	22.70
10:00-10:30	85.75	62.53	120.76	184.06	268.50	270.89	211.00	191.55	167.91	183.04	86.73	47.67
10:30-11:00	134.30	115.33	175.24	236.47	314.50	315.00	258.31	241.22	219.08	230.56	135.05	94.98
11:00-11:30	180.17	167.10	227.78	286.28	356.65	355.53	303.31	288.50	267.55	273.78	181.04	141.02
11:30-12:00	221.76	215.99	276.86	332.21	393.92	391.50	344.88	332.15	311.95	311.45	223.06	183.87
12:00-12:30	257.98	260.49	321.14	373.11	426.16	422.63	381.99	371.08	351.09	343.92	259.75	221.98
12:30-13:00	288.73	299.36	359.71	408.56	452.41	448.27	414.15	404.80	384.94	369.07	291.41	255.04
13:00-13:30	312.04	332.79	392.41	437.81	471.58	467.22	441.07	432.86	412.18	386.08	315.92	281.84
13:30-14:00	327.07	358.74	417.48	459.56	483.11	478.95	461.32	453.80	431.67	394.23	332.36	300.96
14:00-14:30	333.08	376.38	434.18	473.17	486.57	483.03	474.32	467.00	442.74	392.94	339.97	311.56
14:30-14:00	329.39	385.03	441.89	478.12	481.61	479.13	479.62	471.96	444.86	381.64	338.05	312.90
14:00-14:30	315.32	384.06	440.11	474.01	467.99	467.02	476.87	468.27	437.57	359.77	325.94	304.27
14:30-15:00	290.25	372.90	428.38	460.51	445.53	446.55	465.79	455.63	420.45	326.75	302.95	284.94
15:00-15:30	253.70	351.03	406.31	437.35	414.09	417.62	446.21	433.77	393.11	281.84	268.42	254.27
15:30-16:00	185.30	317.95	373.49	404.28	373.49	380.11	417.99	402.45	355.11	210.85	218.80	208.80
16:00-16:30	27.28	273.46	329.62	361.02	323.48	333.86	380.99	361.38	305.84	56.55	75.78	67.04
16:30-17:00	0.00	188.48	273.97	307.24	263.14	278.40	335.00	310.09	238.51	0.02	0	0
17:00-17:30	0.00	16.52	154.15	238.10	176.62	210.46	279.48	245.88	101.73	0	0	0
17:30-18:00	0.00	0.00	2.65	80.19	24.52	91.42	210.68	133.57	4.20	0	0	0
18:00-18:30	0	0	0	0.03	4.13	15.82	15.27	1.83	0	0	0	0
18:30-19:00	0	0	0	0	0	0.04	0.03	0	0	0	0	0

Figure 3: The shading on the 1.44 kW$_c$ installation located at FST at Settat.

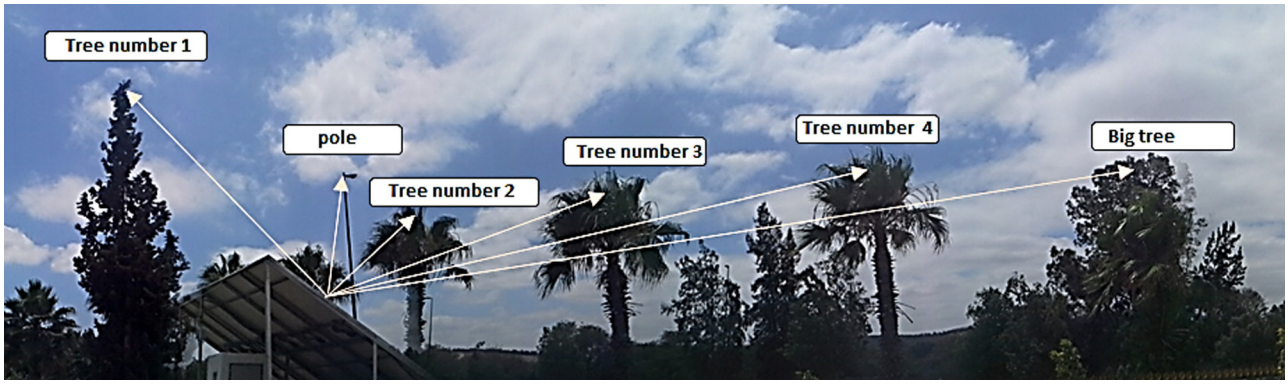

Figure 4: Presence of obstacles (five trees and a pole) in the case of our PV installation.

5.1.2 The objective

Our objective is to study the losses due to shadowing phenomenon on our PV installation. The modules are presented in two strings, and for each string, the modules are wired in series.

In the case of our PV installation in Settat, there are mainly proximity obstacles: five trees and a pole that are shown in Figure 4.

First, we did a study to simulate the annual production of our installation by estimating the losses due to the phenomenon of shading, and then we tried to obtain the same results from the experimental values.

5.2 Survey of the shading mask

The mask survey (shade survey) provides the information needed to calculate these losses. It is necessary to know the expected orientation and inclination of the panels to perform this calculation. They are simple and precise enough that the mask readings can be used in the calculations of production and sizing of a PV field, and one of these methods is using a compass and a clinometer (Schimot et al. 2010).

5.2.1 Materials needed

The tools needed to complete this step are a compass (which will make it possible to measure the azimuth of a point) and a clinometer (for measuring the height of a point).

In the laboratory, we manufactured our own measuring instrument (Figure 5), this method makes it possible to measure the azimuth and the height of a point simultaneously from two rotations (vertical and horizontal) (Schimot et al. 2010).

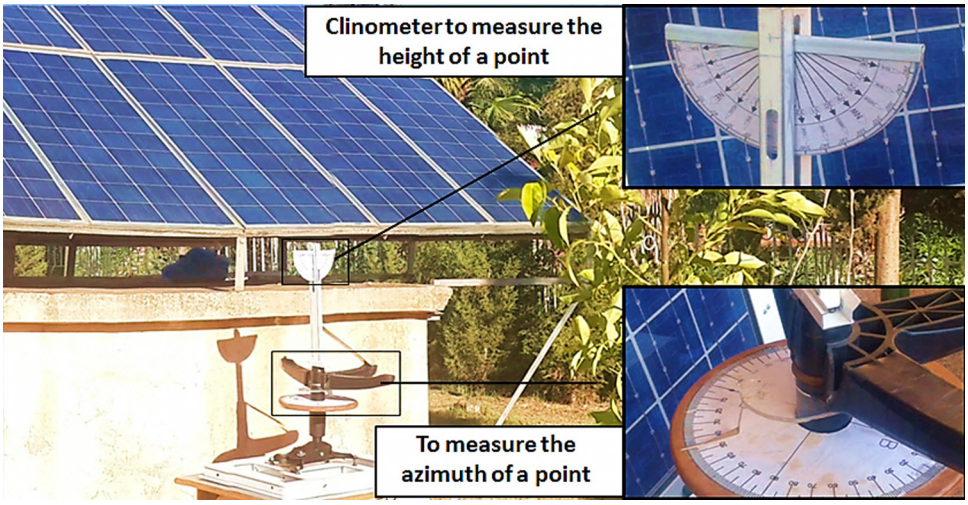

Figure 5: The instrument for measuring elevation and azimuth.

5.3 Identifying the characteristic points of the obstacle geometry

This statement must be made at the level of PV modules. It is therefore up to the roof where the PV modules will be installed, as illustrated in Figure 6. The points of P_1 to P_6 is where the measurements must be made.

Once we are at the point level, we take the compass that indicates the direction of the south, the goal is to define characteristic points of the geometry of the obstacles. For example, for trees and palms it is possible to define characteristic points of its geometry.

5.3.1 Important details

All that is below the modules can never cause shadows on the modules.

5.3.2 Posting the characteristic points on the graph of the race of the sun

Once the characteristic points of the geometric shape of the obstacle is determined, the next step is to post these points on the graph of the solar race. For that, the azimuth and the height of each of the characteristic points defined previously were measured, the azimuth with the compass and the height with the clinometer. For example, let's consider the red point (P3, left image of Figure 6), where "*h*" represents the elevation of each obstacle identified in the vicinity of the installation.

The measurement of the azimuth and the height is to be carried out for all the points defined above. So, we get a table with our surveys. Each tree corresponds to several points, and each point corresponds to an angular height and an azimuth angle. Table 7 represents the angular height as a function of the azimuth angle. With this table we deduced the shadow mask of each obstacle that will be applied to the entire installation.

Then, simply post the points on the graph of the race of the sun, knowing that the abscissa axis of this graph represents the azimuth, and the ordinate axis represents the height.

Table 7: Azimuth angle measurements and angular height of obstacles of our installation

The modules of the first line of our installation		The garden tree	Pole	Tree No 2	Tree No 3	Tree No 4	Big tree
Panel	*D* (m)	10.48	17.75	12.34	8.73	10	56
No 1	*h* (°)	42	33	30	39	39	22
	φ (°)	160	200	215	246	246	294
Panel	*D* (m)	9.82	17.15	11.85	8.57	10.24	56
No 2	*h* (°)	49	38	29	39	36	21
	φ (°)	162	200	219	240	270	295
Panel	*D* (m)	9.16	16.59	11.4	8.44	10.55	56
No 3	*h* (°)	52	38	30	40	23	20
	φ (°)	160	203	220	250	282	296
Panel	*D* (m)	8.5	16	10.86	8.37	10.9	56
No 4	*h* (°)	50	39	255	39	22	19
	AZ (°)	152	220	219	258	290	296
Panel	*D* (m)	7.83	15.45	10.38	8.36	11.27	56
No 5	*h* (°)	60	42	40	38	20	18
	φ (°)	153	210	225	270	300	297
Panel	*D* (m)	7.18	14.9	9.96	8.4	11.72	56
No 6	*h* (°)	62	42	40	30	19	18
	φ (°)	149	220	248	278	320	299

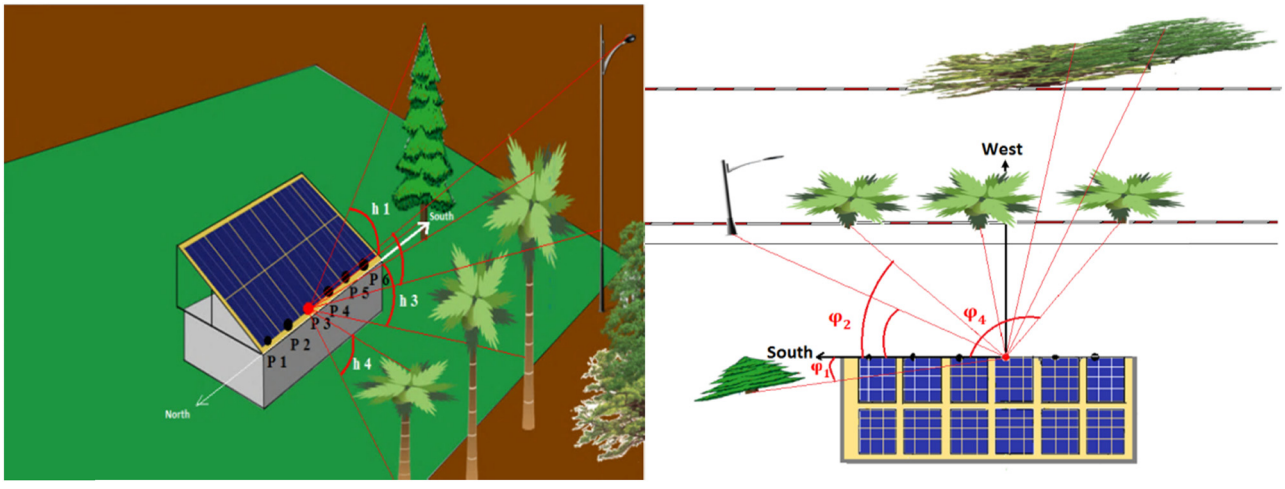

Figure 6: Measuring the height and azimuth of each of the characteristic points.

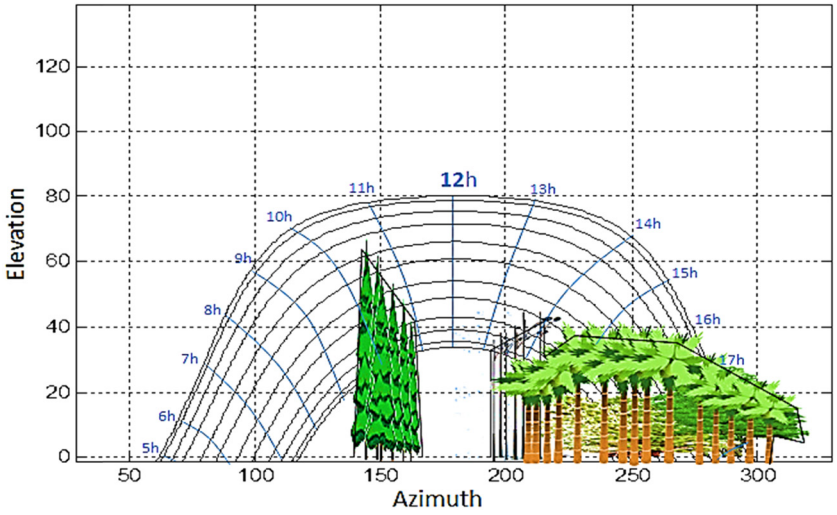

Figure 7: Mask of shadow of the obstacles on the installation.

The measurements of the azimuth and the height of the module point P_3 have made it possible to know the values of (φ and h) of the characteristic points in the shape geometry of the obstacles. These values were then reported in the graph of the sun's course (Figure 7). Upon analyzing the characteristic points of each obstacle, we identify in the mask figure the outlines resembling those of a lamppost, three palm trees, and two trees (the shadows cast by each obstacle onto the PV installation).

The overlying shadow masks for the other PV modules are also shown. We finally obtain the shadow mask that influences the production of all modules of our PV installation (Figure 7).

The effective shadow mask is obtained by the orange surface (Figure 8). This makes it possible to determine the loss coefficient to be applied to the production of the PV field.

In order to calculate the daily solar exposure for each group and line of modules, a comparison of the shadow mask with the sun's trajectory is performed for each hour of a typical day in each month. The sun's trajectory is superimposed with the shadow mask to determine the areas that are shaded by the mask. In these instances, the values of global radiation are replaced with the values of diffuse radiation, and the results are shown in Table 8.

6 Calculation of electricity production

The electrical production of a PV installation obviously depends on the solar irradiation. Therefore, it is impossible to tell in advance how much electricity will be produced by

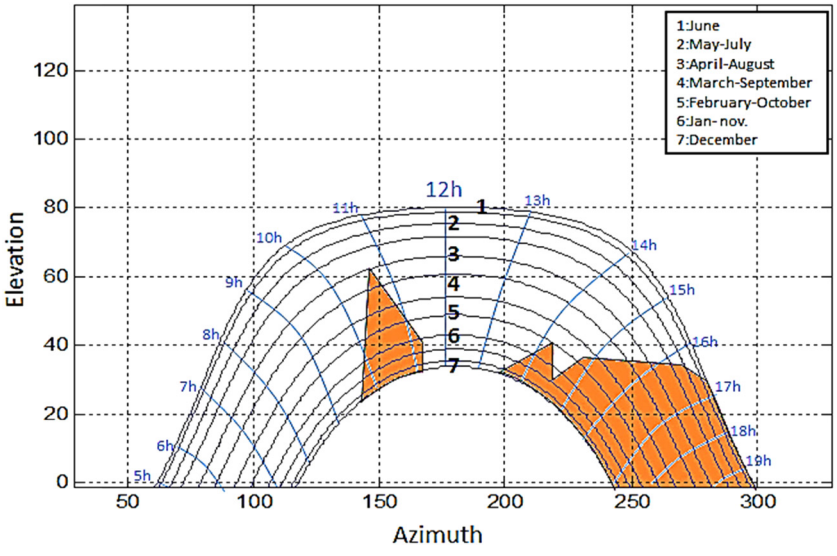

Figure 8: Surface of the drop shadow on the entire installation.

a solar panel without knowing the amount of solar energy received on this panel (Ramaprabha and Mathur 2012, Wang and Hsu 2011) (the production will be different depending on where you install it and even according to the position you give it).

The aim of this section is to assess the electrical output of our installation under both shaded and unshaded conditions. To accomplish this, we will present a straightforward equation to accurately calculate the electrical production of our installation.

So, we have the following relation (Diantari and Pujotomo 2016):

$$E = G \cdot S \cdot \eta_{\text{global}}. \tag{23}$$

The total area of our PV installation was $S = 9.9696\ \text{m}^2$, efficiency of the panel was $\eta_{\text{panel}} = 12\%$, and the performance factor $F_{\text{p}} = 0.8$.

We now calculate the monthly production of the whole of our installation from the previous tables of sunshine (Table 9).

6.1 Calculation of electrical productivity

PV productivity is calculated as the ratio of the power that a PV module provides over a period (1 day, 1 month, or 1 year) to the power produced under the STC standard test conditions (solar irradiation = 1,000 W/m^2, Tcell = 25°C, A.M = 1.5) of the module.

This indicator measures the light intensity of our region, in other words, the yield in kW h per kW_p in an optimal configuration (panels are facing south, at an inclination of 29°). To calculate, we use the equation

Table 8: Representative table of the solar energy received on our PV installation with shading in W h/m^2

	Jan	Feb	Mar	Apr	May	Jun	July	Aug	Sep	Oct	Nov	Dec
05:00-05:30	**0**	**0**	**0**	**0**	**3.15**	**5.32**	**0**	**0**	**0**	**0**	**0**	**0**
05:30-06:00	**0**	**0**	**0**	**0**	**13.89**	**17.87**	**2.38**	**0.04**	**0**	**0**	**0**	**0**
06:00-06:30	**0**	**0**	**0**	**3.82**	**26.24**	**29.64**	**12.84**	**5.53**	**0.69**	**2.27**	**0**	**0**
06:30-07:00	**0**	**0**	**1.98**	**14.28**	**33.91**	**37.09**	**26.49**	**18.41**	**9.00**	**11.36**	**0**	**0**
07:00-07:30	**2.60**	**0.86**	**9.82**	**24.96**	**38.73**	**41.97**	**35.54**	**30.29**	**22.31**	**22.21**	**2.70**	**0**
07:30-08:00	**9.58**	**7.01**	**19.53**	**31.27**	**41.96**	**45.32**	**41.32**	**37.54**	**31.26**	**28.53**	**10.78**	**3.57**
08:00-08:30	**16.19**	**15.68**	**25.52**	**35.08**	**70.57**	**81.75**	**45.23**	**42.16**	**36.55**	**32.27**	**19.14**	**11.18**
08:30-09:00	**19.68**	**20.85**	**28.93**	**39.48**	**119.31**	**128.31**	**68.22**	**47.20**	**39.93**	**36.67**	**23.81**	**17.35**
09:00-09:30	**21.71**	**23.72**	**32.27**	**77.52**	**169.58**	**176.31**	**114.48**	**90.75**	**63.97**	**81.22**	**26.55**	**20.70**
09:30-10:00	**36.56**	**25.72**	**66.20**	**130.51**	**219.78**	**224.27**	**162.59**	**140.87**	**115.59**	**132.67**	**39.03**	*21.72*
10:00-10:30	*23.02*	*26.65*	**120.76**	**184.06**	**268.50**	**270.89**	**211.00**	**191.55**	**167.91**	*37.36*	*29.45*	*23.02*
10:30-11:00	*23.86*	*27.43*	*34.18*	**236.47**	**314.50**	**315.00**	**258.31**	**241.22**	*45.74*	*38.11*	*30.22*	*23.86*
11:00-11:30	*24.41*	**167.10**	**227.78**	**286.28**	**356.65**	**355.53**	**303.31**	**288.50**	**267.55**	**273.78**	*30.71*	*24.41*
11:30-12:00	**221.76**	**215.99**	**276.86**	**332.21**	**393.92**	**391.50**	**344.88**	**332.15**	**311.95**	**311.45**	**223.06**	**183.87**
12:00-12:30	**257.98**	**260.49**	**321.14**	**373.11**	**426.16**	**422.63**	**381.99**	**371.08**	**351.09**	**343.92**	**259.75**	**221.98**
12:30-13:00	**288.73**	**299.36**	**359.71**	**408.56**	**452.41**	**448.27**	**414.15**	**404.80**	**384.94**	**369.07**	**291.41**	**255.04**
13:00-13:30	**312.04**	**332.79**	**392.41**	**437.81**	**471.58**	**467.22**	**441.07**	**432.86**	**412.18**	**386.08**	**315.92**	**281.84**
13:30-14:00	*25.03*	**358.74**	**417.48**	**459.56**	**483.11**	**478.95**	**461.32**	**453.80**	**431.67**	**394.23**	*30.84*	*25.69*
14:00-14:30	*24.73*	**376.38**	**434.18**	**473.17**	**486.57**	**483.03**	**474.32**	**467.00**	**442.74**	**392.94**	*30.39*	*25.35*
14:30-14:00	*24.34*	*28.03*	**441.89**	**478.12**	**481.61**	**479.13**	**479.62**	**471.96**	**444.86**	*37.55*	*29.70*	*24.81*
14:00-14:30	*23.75*	*27.53*	**440.11**	**474.01**	**467.99**	**467.02**	**476.87**	**468.27**	**437.57**	*36.54*	*28.69*	*23.99*
14:30-15:00	*22.87*	*26.80*	**428.38**	**460.51**	**445.53**	**446.55**	**465.79**	**455.63**	**420.45**	*35.12*	*27.23*	*22.80*
15:00-15:30	*21.62*	*25.77*	**406.31**	**437.35**	**414.09**	**417.62**	**446.21**	**433.77**	**393.11**	*33.10*	*25.15*	*21.09*
15:30-16:00	19.81	24.30	30.85	**404.28**	**373.49**	**380.11**	**417.99**	**402.45**	*39.51*	*30.21*	*21.85*	*18.35*
16:00-16:30	*15.59*	*22.22*	*28.83*	*35.90*	*41.91*	**333.86**	*46.84*	*43.71*	*36.21*	*24.45*	*8.33*	*6.33*
16:30-17:00	*2.48*	*16.67*	*25.91*	*32.88*	*38.85*	*42.90*	*43.76*	*40.10*	*30.65*	*7.28*	*0*	*0*
17:00-17:30	*0*	*1.64*	*16.24*	*28.02*	*34.45*	*38.71*	*39.44*	*34.63*	*14.46*	*0*	*0*	*0*
17:30-18:00	*0*	*0*	*0.33*	*10.76*	*25.79*	*32.28*	*32.74*	*20.91*	*0.67*	*0*	*0*	*0*
18:00-18:30	*0*	*0*	*0*	*0*	*4.14*	*15.82*	*15.27*	*1.84*	*0*	*0*	*0*	*0*
18:30-19:00	*0*	*0*	*0*	*0*	*0*	*0*	*0*	*0*	*0*	*0*	*0*	*0*

Bold values: The global Solar irradiation.
Italic values: The diffuse Solar irradiations.

Table 9: Monthly electricity production of our installation for the two modes positions

	Position without shading in kW h/m^2	Position with shading in kW h/m^2
Jan	108.24	42.67
Feb	122.51	62.48
Mar	170.90	136.10
Apr	194.91	169.68
May	218.39	199.31
Jun	216.05	203.12
Jul	218.92	185.83
Aug	204.37	177.08
Sep	172.54	142.19
Oct	143.87	91.92
Nov	109.59	43.20
Dec	99.28	37.29
Whole year	1979.57	1249.62

$$\mathrm{Pr} = \int \frac{P\mathrm{d}t}{P_{\mathrm{stc}}}, \tag{24}$$

where P is the power available at the terminals of the PV panel, P_{stc} is the power of a cell, a module, a system measured in the standard test conditions (Watt-peak-W_c):

- Solar irradiation = 1,000 W/m^2,
- T_{cell} = 25°C,
- A.M = 1.5.

Again, we use a Matlab code to calculate the monthly productivity of our PV installation for both modes of exposure. Finally, we deduce the productivity as shown in Table 10.

Table 10: Monthly productivity of our installation in kW h/kW$_p$

	Position without shading in kW h/kW$_c$	Position with shading in kW h/kW$_c$
Jan	70.58	29.63
Feb	80.08	43.39
Mar	113.27	94.52
Apr	130.74	117.84
May	147.20	138.42
Jun	145.23	141.07
Jul	147.43	129.06
Aug	137.17	122.98
Sep	115.60	98.75
Oct	96.12	63.84
Nov	72.79	30.00
Dec	65.36	25.90
Whole year	1321.57	1035.42

6.2 Results and interpretation

The results of our electrical production calculation reveal a positive correlation between the production at two positions and the angular height of the sun. Specifically, as the solar height angle increases, the production also increases. However, a marked decline in electricity production was observed, with a decrease from 1979.59 kW h for an unshaded position to 1490.87 kW h for a position with shading, resulting in a loss of 24.68%. This decrease is attributed to the shading effect caused by trees and a pole on the PV modules of the installation.

Then, we notice that ridge shading plays a big part in the productivity losses. Previously, for the entire year, with the shade, we obtained a productivity of 1035.42 kW h/kW$_p$. We therefore lost 286.44 kW$_p$ because of the shadow of the ridge, a 22% decrease in productivity compared to the position without shading.

We also notice that the winter months (November, December, January, and February) are the months when productivity is lower, and the losses in winter are greater compared to the other months, this is due to our shadow masks and because of low angular height of the sun in winter in the region of Settat. We find that the lowest percentage loss is in the summer months (May, June, July, and August).

7 Conclusion

The shading effect can have a significant impact on the performance of a PV system, resulting in a decrease in solar power productivity. Thus, it is crucial to identify and mitigate the sources of shading in a PV field. Regular monitoring, at a frequency of quarterly, monthly, weekly, or even daily, is the most effective method to ensure the efficient operation of the PV system and to optimize its performance.

The objective of this article is to provide a precise estimation of the electrical energy output of a PV system, accounting for shading effects. To achieve this, we have conducted comprehensive calculations of the direct and diffuse irradiation received by the PV panels using the Hottel method. Moreover, we have carried out shade mask measurements at various times of the day and a practical study of shading effects using “close shading masks.” By taking shading into account, we can provide an accurate estimation of electricity production in a PV installation, enabling us to optimize the performance of the system.

Acknowledgement: This was a great opportunity for us to be able to prepare this study within the Laboratory of Renewable Energies and Mechanical Optimization "LEROM" at the Faculty of Science and Technology of Hassan 1st University in Settat-Morocco. We would like to thank all the members of the laboratory and all those who helped make this research successful.

Funding information: No funding was received for conducting this study.

Author contributions: Category 1: Conception and design of study: Mohamed NFAOUI, Walid Abouloifa, Sanaa Hayani-Mounir, Khalil El- hami; Acquisition of data: Mohamed NFAOUI, Walid Abouloifa; Analysis and/or interpretation of data: Mohamed NFAOUI, Sanaa Hayani-Mounir, Khalil El-hami. Category 2: Drafting the manuscript: Mohamed NFAOUI, Walid Abouloifa, Mohamed Yassine Roboa; revising the manuscript critically for important intellectual content: Mohamed NFAOUI, Walid Abouloifa, Sanaa Hayani- Mounir, Mohamed Yassine Roboa and Khalil El-hami. Category 3: Approval of the version of the manuscript to be published : Mohamed NFAOUI, Walid Abouloifa, Sanaa Hayani-Mounir, Khalil El-hami.

Conflict of interest: The authors have no conflicts of interest to declare that are relevant to the content of this article.

Data availability statement: The data that support the findings of this study are available from the authors upon reasonable request.

References

Bayraka F., Ertürkb G., and Oztopb H. F. (2017) "Effects of partial shading on energy and exergy efficiencies for photovoltaic panels," *J. Clean. Prod.*, vol. 164, pp. 58–69. doi: 10.1016/j.jclepro.2017.06.108.

Chowdhury S. R. and Saha H. (2010) "Maximum power point tracking of partially shaded solar photovoltaic arrays," *Sol. Energy Mater. Sol. Cell*, vol. 94, pp. 1441–1447. doi: 10.1016/j.solmat.2010.04.011.

Cooper P. I. (1969) "The absorption of solar radiation in solar stills," *Sol. Energy*, vol. 12, no. 3, pp. 333–346. doi: 10.1016/0038-092x(69)90047-4.

Diantari R. A. and Pujotomo I. (2016) "Calculation of electrical energy with solar power plant design," *Int. Semin. Intell. Technol. Its Appl. (ISITIA)*, pp. 443–446. doi: 10.1109/ISITIA.2016.7828701.

Dolara A., Lazaroiu G. C., Leva S., and Manzolini G. (2013). "Experimental investigation of partial shading scenarios on PV (photovoltaic) modules," *Energy*, vol. 55, pp. 466–475. doi: 10.1016/j.energy.2013.04.009.

El Iysaouy L., Lahbabi M., and Oumnad A. (2016). "Etude et comparaison des différentes configurations de Panneaux Photovoltaïques sous l'Effet d'ombrage partiel," *Proc. 5ème Colloque International Environnement et Développement Durable, Rabat, Settat and Kenitra*, https://www.researchgate.net/publication/320002891.

Ennaoui A. (2014) "Photovoltaic solar energy conversion (PVSEC)," *Helmholtz-Zentrum Berlin für Materialien und Energie, Free University of Berlin, Allemand*.

Hashim H. F., Kareem M. M., Al-Azzawi W. K., and Ali A. H. (2021). "Improving the performance of photovoltaic module during partial shading using ANN," *Int. J. Power Electron. Drive Syst.*, vol. 12, pp. 2435–2442, doi: 10.11591/ijpeds.v12.i4.

Islahi A., Shakil S. and Hamed M. (2015) "Hottel's clear day model for a typical arid city – Jeddah," *Int. J. Eng. Sci. Invent.*, vol. 4, no. 6, pp. 32–37.

Kasten F. and Young A. T. (1989) "`Revised optical air mass tables and approximation formula'," *Applied Optics*, vol. 28, pp. 4735–4738. doi: 10.1364/AO.28.004735.

Nfaoui M., and El-hami K. (2018) "Extracting the maximum energy from solar panels," *Energy Rep.*, vol. 41, no. 2, pp. 536–545. doi: 10.1016/j.egyr.2018.05.002.

Nfaoui M., and El-hami K. (2018) "Optimal tilt angle and orientation for solar photovoltaic arrays: case of Settat city in Morocco," *Int. J. Ambient. Energy*, vol. 41, no. 2, pp. 214–223. doi: 10.1080/01430750.2018.1451375.

Nfaoui M., Werzgan, Y., Hayani-Mounir. and El-hami, K. et al. (2023) "Exploring global solar radiation: Enhancing ground-level solar radiation prediction using Hottel's semi-empirical model and sunshine duration analysis," *Int. J. Electr. Eng. Computer Sci.*, vol. 5, pp. 195–204. doi: 10.37394/232027.2023.5.22.

Nfaoui M., Mejdal M., El-Hami K., and Mounir S. H. (2021) "Modeling, simulation and comparison of the photovoltaic productivity by using the MATLAB/PVsystem," *AIP Conference Proceedings*, vol. 2345, p. 020021. doi: 10.1063/5.0049605.

Oudrane A., Aour B., Zeghmati B., Chesneau X., and Messaoud H. (2017) "Étude fondamentale du gisement solaire pour une maison désertique située à ADRAR," *ElWahat Pour les. Rech. et. les Etudes*, vol. 10, no. 2, pp. 136–149.

Ramaprabha R. and Mathur B. L. (2012) "A comprehensive review and analysis of solar photovoltaic array configurations under partial shaded conditions," *Int. J. Photoenergy*, vol. 2012, pp. 1–16. doi: 10.1155/2012/120214.

Sarniak M. T. (2020) "Modeling the functioning of the half-cells photovoltaic module under partial shading in the matlab package," *Appl. Sci.*, vol. 10, no. 7, p. 2575. doi: 10.3390/app10072575.

Schimot Y., Trey A., and Renard G. (2010) "Conception d'un dispositif optique pour l'amélioration de la performance énergétique d'un site de production d'électricité photovoltaïque," *Projet 1004, IUT, 2010*.

Taşçıoğlu A., Taşkın O., and Vardar A. (2016) "A power case study for monocrystalline and polycrystalline solar panels in Bursa City, Turkey," *Int. J. Photoenergy*, vol. 2016, p. 7. doi: 10.1155/324138.

Tiwari G. N. (2004) *Solar energy, fundamentals, design, modeling and applications*. New Delhi, India, Narosa Publishing House.

Tiwari G. N. and Barnwal P. (2008) *Fundamentals of solar dryers*. New Delhi, India, Anamaya Publishers.

Vasiliev M., Nur-E-Alam M., and Alameh K. (2019). "Initial field-testing results from building-integrated solar energy harvesting windows installation in Perth, Australia," *Appl. Sci.*, vol. 9, no. 19, p. 4002. doi: 10.3390/app9194002.

Wang Y. J. and Hsu P. C. (2011) "An investigation on partial shading of PV modules with different connection configurations of PV cells," *Energy*, vol. 36, no. 5, pp. 3069–3078. doi: 10.1016/j.energy.2011.02.052.